



Single and mixed adsorption of Cd(II) and Cr(VI) onto citrate-coated magnetite nanoparticles

M.J. Silva-Silva^a, O.F. Mijangos-Ricardez^a, V. Vázquez-Hipólito^b, S. Martínez-Vargas^{c,*}, J. López-Luna^{a,*}

^a*Instituto de Estudios Ambientales, Universidad de la Sierra Juárez, Ixtlán de Juárez, Oaxaca, 68725, Mexico, Tel. +52 9515536362; Fax: +52 9515536364; email: jlol_24@hotmail.com (J. López-Luna)*

^b*Centro de Investigación en Matemáticas, A. C., Guanajuato, 36000, Mexico, Tel. +52 4737327155; Fax: +52 4737325749*

^c*Facultad de Ingeniería, Universidad Autónoma del Carmen, Ciudad del Carmen, Campeche, 24115, Mexico, Tel. +52 9383811018, ext. 1702; Fax: +52 9383811018, ext. 1328; email: sergelio@gmail.com (S. Martínez-Vargas)*

Received 5 February 2014; Accepted 14 November 2014

ABSTRACT

In the present work, we compared single and mixed adsorption of Cd(II) and Cr(VI) onto co-precipitation synthesized citrate-coated magnetite nanoparticles (NPs). Single kinetic studies revealed Cr(VI) to be better adsorbed than Cd(II). Otherwise, Cd(II) adsorption ratio was improved with Cr(VI) in the binary mixture. Single and mixed adsorption data followed in good agreement the pseudo-second-order kinetic model, with higher initial adsorption rate and rate constant values for Cr(VI). Equilibrium data from single Cd(II) and Cr(VI) adsorption only fitted concordantly the Freundlich isotherm model. The sorption capacity of magnetite NPs as function of initial metal concentrations was found to be 3 mg/g for Cd(II) and 4.65 mg/g for Cr(VI).

Keywords: Cd(II); Cr(VI); Magnetite NPs; Adsorption; Pseudo-second-order model; Freundlich isotherm

1. Introduction

Cadmium is a toxic heavy metal that has been released to the environment through the combustion of fossil fuels, metal production, phosphate fertilizers application, electroplating, and the manufacturing of batteries, pigments, and screens; exerting serious contamination of both soil and water [1]. In human beings, cadmium causes health problems such as damage to kidneys and lung tissues, emphysema, and carcinogenesis [2]. At many sites, chromium has been entering the environment via leakage, poor storage, or

unsafe disposal practices [3] like that of leather industries whose tannery wastes greatly contribute to the total industrial chromium pollution [4]. Cr oxidation states vary between -2 and $+6$, but only the $+3$ and $+6$ states are stable under commonly observed environmental conditions [5]. Hexavalent chromium is a known human carcinogen and is mobile, whereas trivalent chromium is comparatively less toxic and relatively immobile [6]. Moreover, cadmium and chromium are included in the current US-EPA List of 126 Priority Pollutants [7] where drinking water regulations have established 0.005 mg/L maximum contaminant level (MCL) for cadmium and 0.1 mg/L for total chromium [8].

*Corresponding authors.

Several methodologies are currently available for heavy metal removal from water, but adsorption has gained importance as a purification and separation process using different types of adsorbent materials [9]. Nano-iron oxides from different chemical species have been proven to be useful adsorbents of heavy metals [10–14]. Goethite, hematite, magnetite, and ferri-rite are the materials more extensively used for heavy metal removal from water, being magnetite the most efficient iron oxide [15]. Additionally, magnetite can be easily separated from heavy metal solution using a soft magnetic field. On the other hand, most reports from the literature deal with the adsorption of single heavy metals onto magnetite nanoparticles (NPs), but studies of mixed metals are scarce. Accordingly, the aim of this work was to compare the adsorption kinetics of single Cd(II) and Cr(VI) and binary mixtures of the metals, using synthesized sodium citrate-coated magnetite NPs. As is known, the hydrophilic group of citrate provides an important role in the preparation of Fe₃O₄ NPs. The citrate ions are immobilized on the NP surface, since three carboxyl groups in each citrate ion generate forces between the electric charges of the radical ions of the magnetite NPs to protect them from oxidation. Likewise, the chelation of iron ions by citrate prevents nucleation, thus decreasing the size of magnetite NPs [16,17] and consequently, increasing their specific surface area. An additional fact is that citrate ions improve magnetite NPs solubility in water, thereby improving the heavy metal removal capacity.

2. Materials and methods

2.1. Magnetite synthesis

Magnetite was synthesized by the modified coprecipitation Massart's method [18]. 8 mmol Fe₂(S-O₄)₃·H₂O (Fermont) was dissolved in 10 mL deionized water acidified with 4 mL HCl 1.0 N, and then, 4 mmol FeSO₄·7H₂O (J.T. Baker) was added. After complete dissolution, 100 mL NaOH 3.0 M was dropwise added under vigorous stirring. Precipitated magnetite was rinsed thrice with deionized water by soft magnetic decantation. Afterwards, 50 mL of sodium citrate 4.0 mM was added maintaining 30 min at 80°C on continuous stirring. Magnetite was rinsed thrice again and in the last rinsing pH was adjusted to 5.5 with HCl 0.1 N. Finally, magnetite was dried at 45°C.

2.1.1. Magnetite characterization

Magnetite NPs were characterized by powder X-ray diffractometry (XRD), Fourier transform infrared spectroscopy (FTIR), magnetometry and transmission

electron microscopy (TEM). For powder XRD, a Philips X'Pert diffractometer (Cu K α radiation, $\lambda = 0.15418$ nm) was used, where the diffractogram from the citrate-coated magnetite sample was compared to the Power Diffraction File (PDF) database to determine the iron oxide phase of the particle. The infrared spectra were recorded in the range 400–4,000 cm⁻¹ on a FTIR NICOLET 5700 spectrometer. A sample of citrate-coated magnetite NPs (1 mg) was mixed in 30 mg KBr according to the specifications of the infrared spectrometer.

Magnetometry analysis was conducted by magnetic hysteresis at room temperature (300 K) using an AGM Micromag 2900 Magnetometer. For TEM determination (CIQA, Saltillo, México), a minimal dust magnetite NPs sample was suspended in 350 μ L of acetone and dispersed in an ultrasonic bath for 30 min. Then, a middle droplet from the dispersion was placed in a lacey carbon-supported copper grid. The grid was completely dried before being introduced in the microscope (FEI 80–300 Microscope Schottky-type, 0.14 nm point-to-point resolution, 1.25 mm Cs, 300 kV). Conventional, HRTEM and SAED NPs images were obtained.

2.2. Cd(II) and Cr(VI) adsorption kinetics

For single adsorption experiments, Cd(II) and Cr(VI) solutions (1, 2.5, 5, 7.5, and 10 mg/L) were prepared with deionized water and adjusted to pH 5.5 with 0.1 N HCl. Cd(II) and Cr(VI) were obtained from Cd(NO₃)₂·4H₂O (J.T. Baker) and K₂Cr₂O₇ (Fermont), respectively. For binary adsorption experiments, the three different treatments (1–10, 5–5, and 10–1 mg/L Cd–Cr) were prepared as stated before.

The kinetics of the heavy metals adsorption was developed varying the contact time between magnetite NPs (1 g/L) and solutions, from 5 to 180 min. Thus, 0.01 g of magnetite NPs was placed in 30-mL polyethylene flasks, and then, 10 mL of Cd(II), Cr(VI), or binary solution was added. The flasks were shaken at 300 rpm on a LabGenius oscillatory shaker and progressively retired after 5, 10, 15, 30, 60, 120, and 180 min. Then, the complete samples from each flask were soft magnetic decanted, filtered through Whatman #42 ashless circles, and acidified with nitric acid for heavy metal determination by ICP–OES [19], Perkin Elmer Optima 7000 DV. All experiments were conducted at room temperature (20°C).

The metal adsorption over time (mg/g) was calculated by the following equation:

$$q_t = (C_0 - C_t) \frac{V}{m} \quad (1)$$

where C_0 (mg/L) is the initial metal solution concentration, C_t (mg/L) is the metal concentration after shaking time, V (L) is the volume of the solution, and m (g) is the adsorbent weight.

2.3. Pseudo-second-order kinetic model

Since indeterminate values prevented the pseudo-first-order model [20] or the fractional power model [21] to be applied, single and binary Cd(II)–Cr(VI) adsorption data were fitted using the pseudo-second-order kinetic model [1]:

$$\frac{t}{q_t} = \frac{1}{k_2 q_e^2} + \frac{1}{q_e} t \quad (2)$$

where k_2 (g/mg min) is the rate constant and $k_2 q_e^2$ or h (mg/g min) is the initial adsorption rate; q_e and k_2 were obtained from the slope and the intercept plotting t/q_t vs. t . Chi-square test (χ^2) was used as error function to measure the difference between experimental and model calculated data:

$$\chi^2 = \frac{(q_{e, \text{exp}} - q_{e, \text{cal}})^2}{q_{e, \text{cal}}} \quad (3)$$

2.4. Adsorption isotherm

Single Cd(II) and Cr(VI) adsorption equilibrium data were fitted using Langmuir, Freundlich, Tempkin, Redlich–Peterson, Toth, Koble–Corrigan, and Khan isotherm models, broadly discussed by Foo and Hameed [22]. However, equilibrium data only fitted the Freundlich model:

$$q_e = K_F C_e^n \quad (4)$$

where K_F (L/g) reflects adsorbent capacity and n (unitless) is the heterogeneity factor, since Freundlich isotherm describes heterogeneous surfaces and does not assume monolayer capacity [9]. K_F and n were obtained from nonlinear least-square method using Matlab ver. 7.10.0. Sum square error (ERRSQ) was used as error function. By the same way, sorption capacity was calculated as function of initial concentrations and equilibrium adsorption.

2.5. Statistical analysis

An analysis of variance (ANOVA) and LSD comparison method were conducted to determine significant differences among treatments in single and

binary Cd(II) and Cr(VI) adsorption, over contact time with magnetite NPs. A t -test paired method was applied for adsorption comparison between single and binary mixture treatments. Additionally, Pearson's correlation analyses were developed to establish any relationship between Cr(VI) and Cd(II) adsorption in the binary mixture. Statistical analyses were performed with the SAS System Software ver. 9.0 at $p < 0.05$.

3. Results and discussion

3.1. Magnetite NPs characterization

The XRD patterns of citrate-coated magnetite NPs matched very well with the spinel structure of Fe_3O_4 (JCPDS card No. 89–691). This result confirmed the formation of a pure magnetite NPs phase (Fig. 1).

Fig. 2 shows the FTIR spectra of the citrate-coated magnetite NPs. The vibration bands for the sodium citrate are found to be rather broad band at 580 cm^{-1} , which is believed to be associated with the stretching vibrations of the tetrahedral groups ($\text{Fe}^{3+}-\text{O}^{2-}$) for Fe_3O_4 . Peaks corresponding to stretching modes ν (asymmetrical, COO^-), ν (symmetrical, COO^-) and ν (CH) of citrate appeared at 1,629, 1,383, and $1,054 \text{ cm}^{-1}$, respectively, indicating the citrate molecules have been adsorbed on the surface of NPs.

The hysteresis cycle of the citrate-coated magnetite NPs (Fig. 3) revealed magnetization saturation (M_s) slightly higher than 40 emu/g , confirming a super

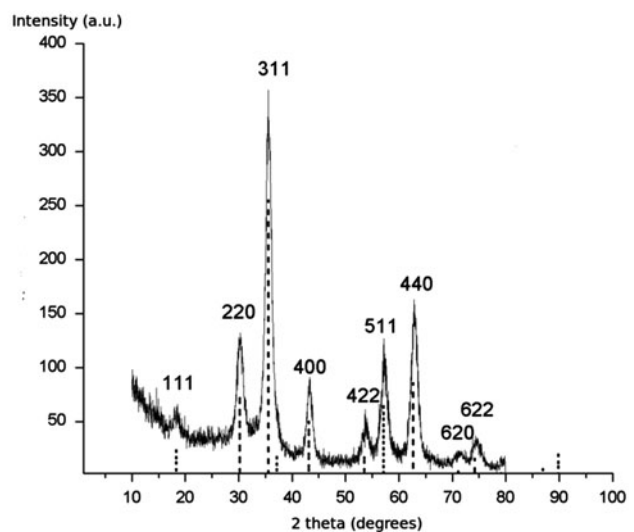


Fig. 1. X-ray diffraction patterns of citrate-coated magnetite NPs. The discontinued lines indicate the Fe_3O_4 diffractions of the cubic spinel structure (JCPDS card No. 89-691).

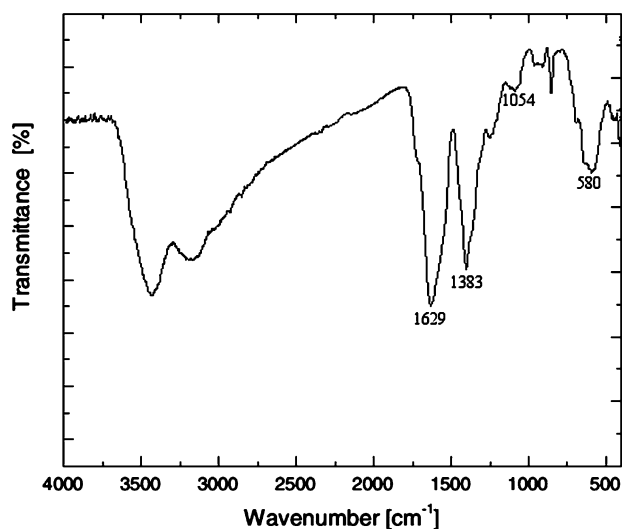


Fig. 2. FTIR spectra of the citrate-coated magnetite NPs.

paramagnetic NP, characteristic property of a soft ferromagnetic material-like magnetite [23]. The synthesized particles analyzed by TEM were found on the nanometric scale, with polydisperse and polymorphic properties (Fig. 4). In general, the NPs mainly contain cubic particles with square sides ranging from 10 to 20 nm, spherical particles 2–10 nm, and rod shaped particles above 40 nm in lesser ratio. Because of the magnetic nature of the sample, NPs aggregation conducted to agglomerates formation.

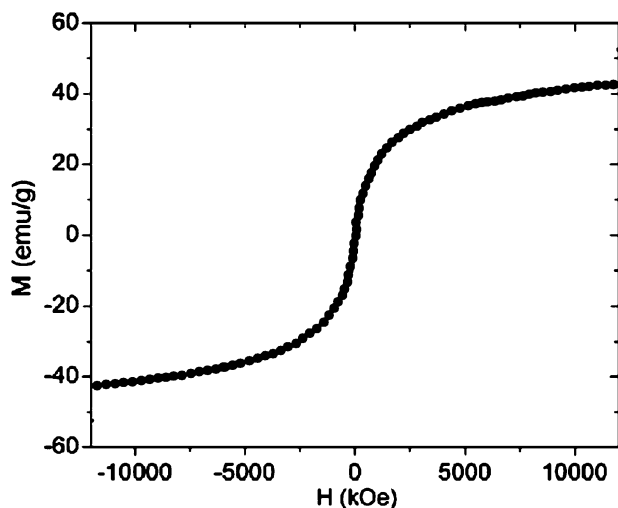


Fig. 3. Magnetization curves of citrate-coated magnetite NPs determined at room temperature.

3.2. Adsorption kinetics

3.2.1. Single treatments

For comparison proposal between single and binary adsorption kinetics, only three concentration treatments are shown (Fig. 5). Single Cr(VI) at 1 mg/L initial concentration was rapidly adsorbed remaining almost constant after 30 min in contact with magnetite NPs. Adsorption ratio was observed to increase over time at 5 and 10 mg/L treatments, reaching equilibrium between liquid and solid phase at 120 min. As initial Cr(VI) concentration was increased similar kinetic trends were appreciated, but even though no remarkable differences in Cr(VI) adsorption were observed, significant statistical differences were actually recorded (LSD test, $p < 0.05$).

Lower concentrations of single Cd(II) were importantly adsorbed onto citrate-coated magnetite NPs. However, as treatments increased, maximal adsorption concentrations reached at 30 min constantly diminished until equilibrium conditions at 120 min. Adsorption was found to be proportional to initial Cd(II) concentrations, with significant differences among treatments (LSD test, $p < 0.05$). Cr(VI) was slightly better adsorbed than Cd(II).

3.2.2. Binary mixture

Better trend was observed for Cr(VI) adsorption in the binary mixture (Fig. 6). However, increasing initial Cr(VI) concentrations in the presence of Cd(II) not

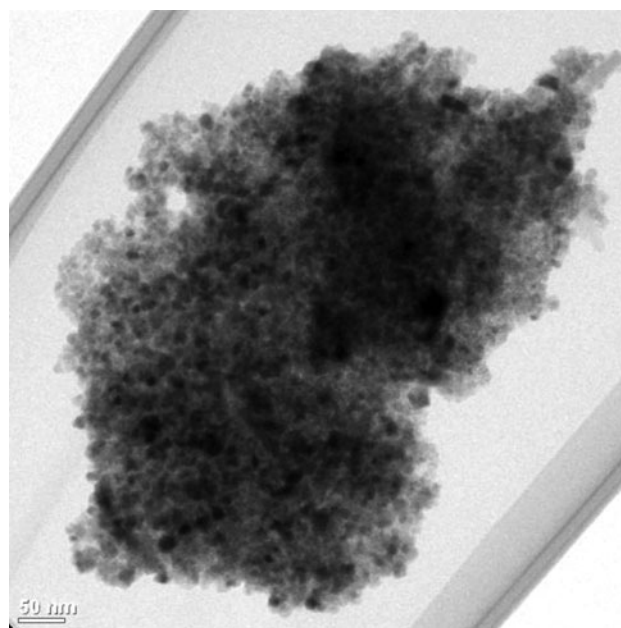


Fig. 4. TEM image showing citrate-coated magnetite NPs.

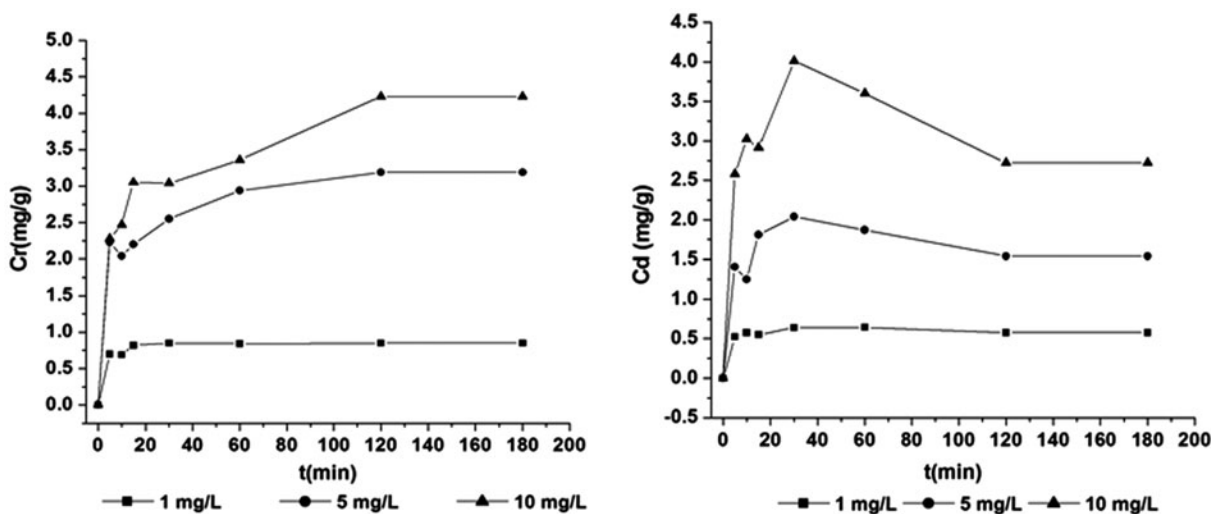


Fig. 5. Single Cr(VI) and Cd(II) adsorption kinetics conducted at room temperature (20°C), 1 g/L citrate-coated magnetite NPs, pH 5.5, and 300 rpm.

necessarily represented important increase in Cr(VI) adsorption, in spite of significant differences recorded among treatments (LSD test, $p < 0.05$). When Cr(VI) was added, the Cd(II) adsorption trend was improved for lower concentrations. The higher initial Cd(II) concentration still was found difficult to achieve equilibrium conditions, as the single treatments. Significant differences (LSD test, $p < 0.05$) among treatments were also recorded. The Pearson's correlation analysis ($r 0.95$, $p < 0.05$) demonstrated the adsorption improvement when the mixture contained equal Cd(II) and Cr(VI) initial concentrations. For different binary initial concentrations of the metals, any correlation was observed.

The paired t -test comparison analysis between single and binary treatments revealed that Cr(VI) adsorption in the mixture was not affected by the Cd(II) presence ($t 0.35$, $p > 0.05$); in fact, Cr(VI) in the binary

mixture was adsorbed in the same extent that Cr(VI) in the single treatments. Conversely, Cd(II) was positively affected by Cr(VI) in the binary mixture ($t -2.84$, $p < 0.05$), being its adsorption increased as compared to single treatments. This could be due to the fact that protonated and positively charged sorbent surface attracts negatively charged chromate ions [24]; being Cd in turn, electrostatically attracted to this complex, enhancing its adsorption. Otherwise, highly protonated surfaces are not favorable for cadmium uptake as Cd^{++} is the dominant ion [25].

3.3. Pseudo-second-order kinetic model for single and binary mixture adsorption

It has been observed that with high initial solute concentrations, the adsorption kinetic better fits the pseudo-first-order model, maintaining a linear

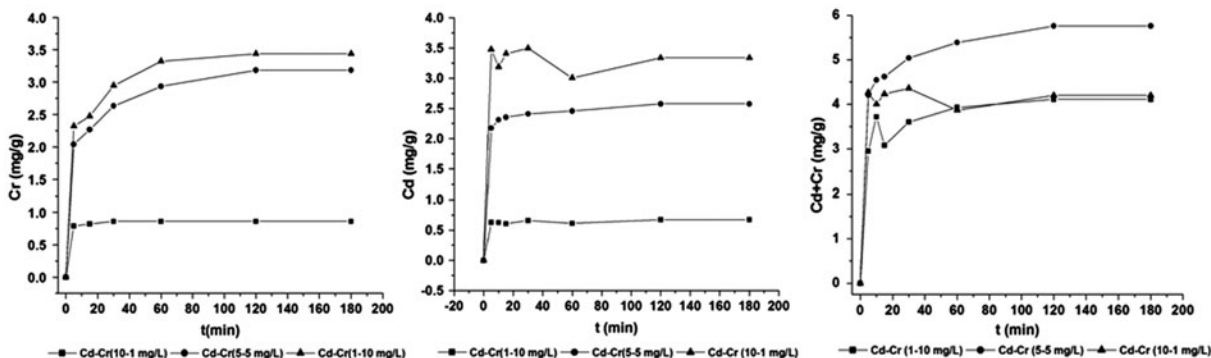


Fig. 6. Binary Cr(VI) and Cd(II) adsorption kinetics conducted at room temperature (20°C), 1 g/L citrate-coated magnetite NPs, pH 5.5, and 300 rpm.

relationship between the rate constant and initial concentration [26]. Conversely, not too high initial concentrations better fit the pseudo-second-order model, with the rate constant in complex function with initial concentrations [26]. Accordingly, in our research, single and binary Cd(II)–Cr(VI) adsorption followed in good agreement the pseudo-second-order kinetic model (Figs. 7 and 8), as it was demonstrated by the high linear regression coefficients (Table 1).

In single treatments, the initial adsorption rate (h) and the rate constant (k_2) diminished with increasing Cr(VI) concentrations (Table 1). Negative rates were recorded for Cd(II) since it can be observed in Fig. 5 that the highest adsorption values achieved at 5 min in contact with citrate-coated magnetite NPs were progressively diminished until reaching equilibrium conditions. In comparison with single treatments, higher initial adsorption rates were recorded for Cd(II) and Cr(VI), individually examined in the binary mixture. The initial adsorption rate increase in the total mixture corresponded to increasing Cd(II) and decreasing Cr(VI) treatments concentrations.

Analyzing Cr(VI) and Cd(II) separately in the binary mixture, it could be observed that the highest rate constants corresponded to 10–1 and 1–10 Cd–Cr treatments (2.638 and 0.880 g/mg min, respectively). Meaning the rate constants to be increased by the rapid diffusion of the lowest initial Cr(VI) and Cd(II) concentrations (1 mg/L) but remarkably decreased for the equal Cd–Cr initial concentration treatment. Findings indeed corroborated by the rate constant values in the total binary mixture. Such behavior was expected, since the adsorption mechanism involves external mass transfer of solute molecules from the solution bulk to the sorbent particle surface, succeeded by

diffusion within the particle internal structure to the sorption sites where rapid uptake occurs, but being the intraparticle diffusion the main course of adsorption [9].

As stated before, Cd(II) adsorption was more extensive in Cr(VI) presence and beyond, at equal initial concentrations. The pseudo-second-order kinetic model resulted very reliable to predict equilibrium adsorption (q_e) as very small differences (χ^2) were observed between calculated and experimental data. The pseudo-second-order rate expression assumes that metal ions like cadmium are chemisorbed onto more than one sorption site on the sorbent surface [1]. Our adsorption kinetic data very well fitted the pseudo-second-order model, suggesting chemisorption of Cd(II) and Cr(VI) onto magnetite NPs. Accordingly, Boparai et al. [1] found such trends when adsorbing cadmium onto nano-zero valent iron NPs (ZVI NPs). Similar trends were also recorded with Cd(II) adsorption using others adsorbents such as chitin [27], orange waste [28], dried activated sludge [29], and mixed maghemite–magnetite NPs [30]. Additionally, the pseudo-second-order model was profitable applied using Bi_2O_3 [31] and calcined Mg–Al– CO_3 hydrotalcite [32] as Cr(VI) adsorbents. Thus, it should be highlighted that the pseudo-second-order model is being applied for analysis of sorption kinetics from liquid solutions since a few years ago [1,26,30,31,33].

3.4. Freundlich isotherm for single Cr(VI) and Cd(II) adsorption

Cr(VI) better fitted the Freundlich isotherm model (Fig. 9) than Cd(II), since adsorption kinetics discussed previously, showed higher adsorption ratio for Cr(VI).

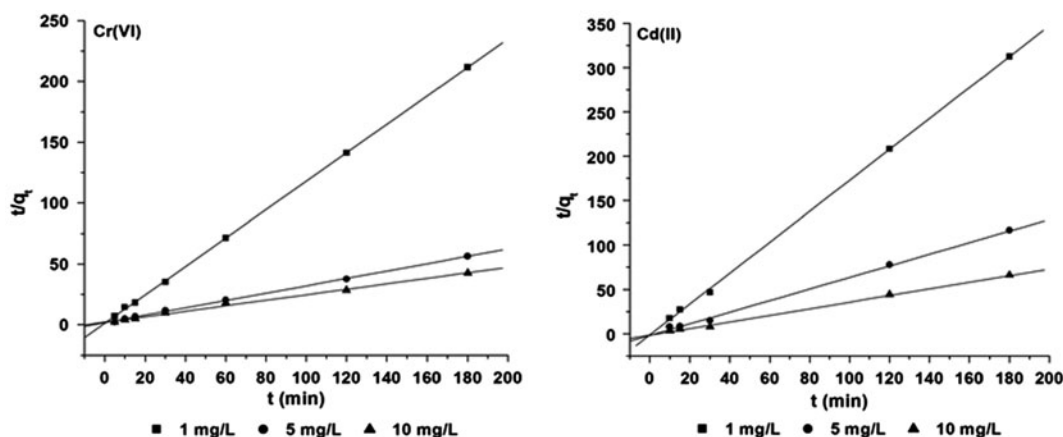


Fig. 7. Pseudo-second-order kinetics of single Cr(VI) and Cd(II) sorption onto citrate-coated magnetite NPs. Kinetic parameters are shown in Table 1.

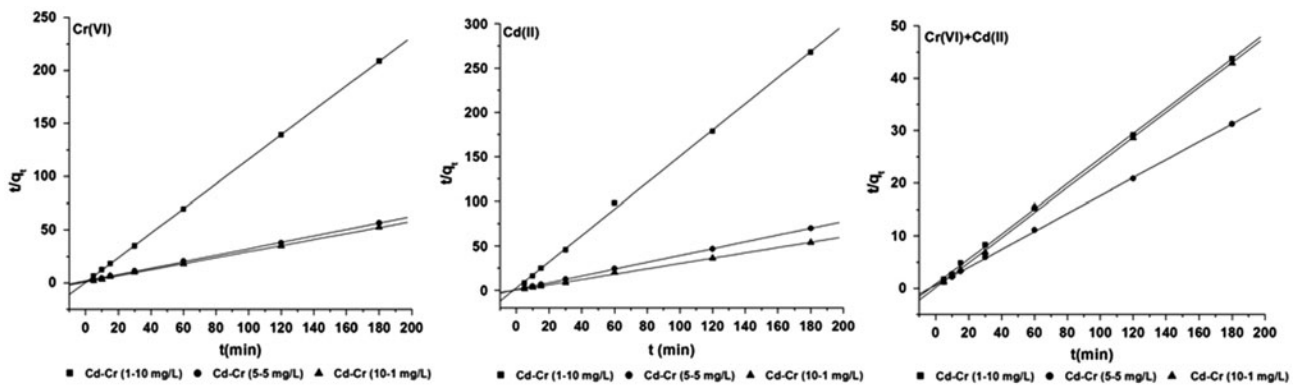


Fig. 8. Pseudo-second-order kinetics of binary Cr(VI) and Cd(II) sorption onto citrate-coated magnetite NPs. Kinetic parameters are shown in Table 1.

Table 1
Pseudo-second-order kinetic parameters for single and binary Cr(VI) and Cd(II) adsorption

Ion	Treatment (mg/L)	h (mg/g min)	k_2 (g/mg min)	R^2	q_e cal (mg/g)	q_e exp (mg/g)	Chi^2 (X^2)
<i>Single</i>							
Cr	1	0.763	1.045	0.9998	0.855	0.850	2.58×10^{-5}
	5	0.532	0.048	0.9990	3.333	3.190	6.2×10^{-3}
	10	0.465	0.023	0.9940	4.545	4.230	2.2×10^{-2}
Cd	1	-0.465	-1.408	0.9984	0.575	0.576	2.88×10^{-6}
	5	-0.532	-0.225	0.9950	1.538	1.540	1.46×10^{-6}
	10	-0.599	-0.082	0.9924	2.703	2.720	1×10^{-4}
<i>Mixture</i>							
Cr	Cd-Cr 10-1	1.961	2.638	1	0.862	0.862	5.52×10^{-9}
	5-5	0.592	0.053	0.9992	3.333	3.232	6.7×10^{-3}
	1-10	0.926	0.073	0.9992	3.571	3.438	5×10^{-3}
Cd	1-10	0.402	0.880	0.9990	0.676	0.672	1.99×10^{-5}
	5-5	1.493	0.216	0.9998	2.632	3.184	1.8×10^{-3}
	10-1	5.263	0.474	0.9984	3.333	3.438	6.53×10^{-6}
Cd-Cr	1-10	1.250	0.072	0.9994	4.167	4.110	7.7×10^{-4}
	5-5	1.613	0.047	0.9996	5.882	5.760	2.5×10^{-3}
	10-1	7.143	0.411	0.9990	4.167	4.200	2.7×10^{-4}

The Freundlich model can be applied to multilayer adsorption, with non-uniform distribution of adsorption heat and affinities over the heterogeneous surface, and then, the amount adsorbed is the summation of adsorption on all sites (each having bond energy), with the stronger binding sites are occupied first, until adsorption energy is exponentially decreased upon the completion of adsorption process [22].

Accordingly and as early mentioned, the synthesized magnetite NPs in the present work were found polymorphic and polydisperse, in agreement with the recorded n values (Table 2) suggesting heterogeneous

adsorbent surfaces. Adsorbent capacity values (K_F) showed Cr(VI) to be more strongly attracted to magnetite NPs than Cd(II), since larger K_F and n values reflect high affinity between adsorbate and adsorbent, and are indicative of chemisorption [1].

It should be considered that isotherms parameters are greatly dependant on initial heavy metal concentrations and laboratory experimental conditions. Thus, increasing the adsorbent dosage implies higher heavy metal removal, but lower adsorption capacity. Conversely, by diminishing adsorbent dosage, the heavy metal removal is impaired, but adsorption capacity is

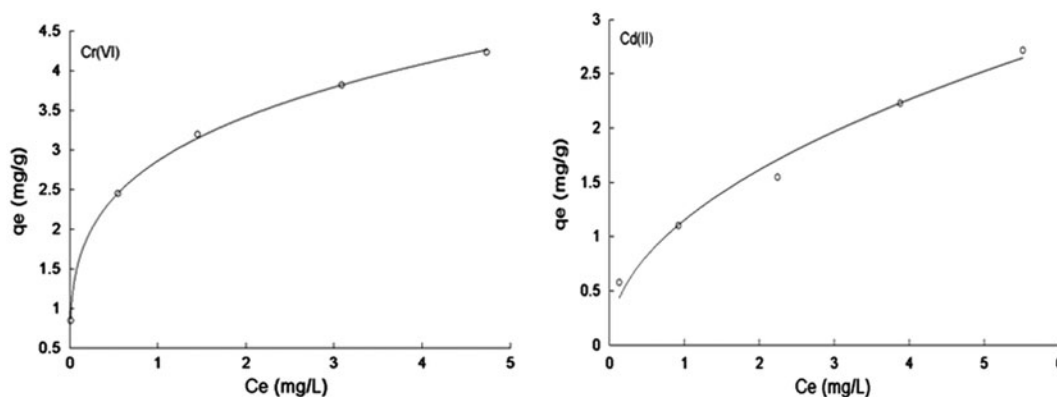


Fig. 9. Freundlich isotherms for Cr(VI) and Cd(II) adsorption onto citrate-coated magnetite NPs.

Table 2

Summary of Freundlich isotherm and sorption capacity constants for Cr(VI) and Cd(II) adsorption onto citrate-coated magnetite NPs

Freundlich isotherm					Sorption capacity as function of initial concentrations		
Ion	Nonlinear model	K_F (L/g)	n	ERRSQ	Sorption equation	ERRSQ	Capacity (mg/g)
Cr	$q_e = 2.85C_e^{0.26}$	2.85	0.26	0.0043	$q_e = 1.28C_o^{0.56}$	0.20	4.65
Cd	$q_e = 1.15C_e^{0.49}$	1.15	0.49	0.0510	$q_e = 0.71C_o^{0.63}$	0.018	3.03

remarkably increased. As it was observed for Cd(II) adsorption onto mixed maghemite–magnetite NPs [29].

Although direct comparison of magnetite NPs with other adsorbents is difficult due to the different experimental conditions applied, in the present work (Fig. 10, Table 2), the magnetite NPs adsorption capacity (3 mg/g) for Cd(II) was higher than that reported for hematite (0.24 mg/g) [25], but slightly lower than other adsorbent like activated carbon (3.37 mg/g) [34].

Namdeo and Bajpai [35] reported 1.53, 3.07, and 3.96 mg/g Cr(VI) adsorption capacity at pH 2 and 30, 40, and 50°C, respectively, when using co-precipitation synthesized magnetite NPs. In this study, the magnetite NPs adsorption capacity for Cr(VI) was found to be 4.65 mg/g, highly competitive, since our experiments were conducted in a less favorable adsorption scenario.

Even though Cd(II) and Cr(VI) uptake could be increased by pH optimization, in the present work,

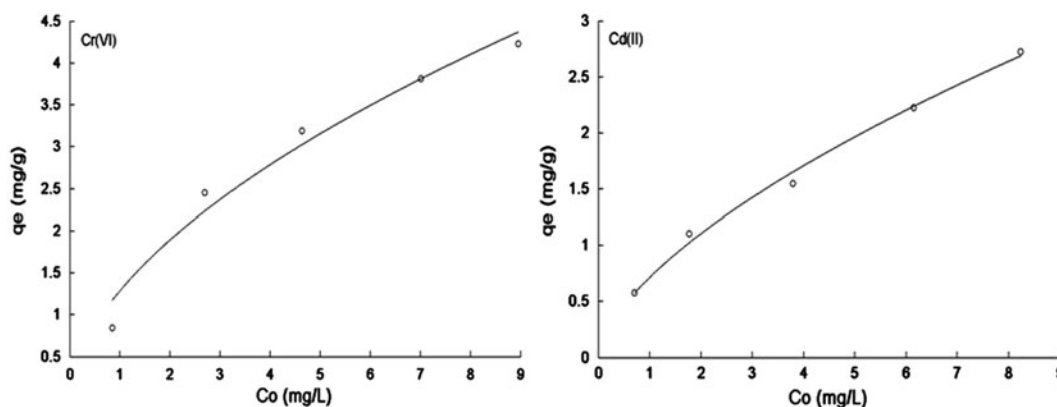


Fig. 10. Magnetite sorption capacity of Cr(VI) and Cd(II) as function of initial concentrations.

the heavy metal adsorption was carried out at pH 5.5, which is representative of several natural ground waters [36].

4. Conclusions

Although the synthesized citrate-coated magnetite NPs were found to be polymorphic and polydisperse, they were shown to be useful for Cd(II) and Cr(VI) removal from water. Cr(VI) resulted more strongly attracted to magnetite NPs, but in the binary mixture Cd(II) uptake was improved by Cr(VI). Adsorption data of both heavy metals fitted in very good agreement the pseudo-second-order kinetic model and the Freundlich isotherm model.

Acknowledgements

This work was former financially supported by F-PROMEP-38/Rev-03 SEP-23-005 and then CAUP-2EA-1115, SEP- CONACYT CB-2010-157232, and SEP-CONACYT CB-2012-01 181592.

References

- [1] H.K. Boparai, M. Joseph, D.M. O'Carroll, Kinetics and thermodynamics of cadmium ion removal by adsorption onto nano zerovalent iron particles, *J. Hazard. Mater.* 186 (2011) 458–465.
- [2] F.A. Solís-Domínguez, M.C. González-Chávez, R. Carrillo-González, R. Rodríguez-Vázquez, Accumulation and localization of cadmium in *Echinochloa polystachya* grown within a hydroponic system, *J. Hazard. Mater.* 141 (2007) 630–636.
- [3] S.R. Chowdhury, R.E.K. Yanful, Arsenic and chromium removal by mixed magnetite-maghemite nanoparticles and the effect of phosphate on removal, *J. Environ. Manage.* 91 (2010) 2238–2247.
- [4] M. Barajas-Aceves, J. Corona-Hernández, R. Rodríguez-Vázquez, Chromium fractionation in semi-arid soils amended with chromium and tannery sludge, *J. Hazard. Mater.* 146 (2007) 91–97.
- [5] S. Avudainayagam, M. Megharaj, G. Owens, R.S. Kookana, D. Chittleborough, R. Naidu, Chemistry of chromium in soils with emphasis on tannery waste sites, *Rev. Environ. Contam. Toxicol.* 178 (2003) 53–91.
- [6] A. Yassi, E. Nieboer, Carcinogenicity of chromium compounds, in: J.O. Niragu, E. Nieboer (Eds.), *Chromium in Natural and Human Environments*, Wiley, New York, NY, 1988, pp. 443–495.
- [7] Environmental Protection Agency, *Water: CWA Methods, Priority Pollutants*, USA. Available from: <<http://water.epa.gov/scitech/methods/cwa/pollutants.cfm>>. Consulted Jan 22, 2014.
- [8] Environmental Protection Agency, *National Primary Drinking Water Regulations*, EPA 816-F-09-004, Washington, DC, 2009.
- [9] G. McKay, *Use of Adsorbents for the Removal of Pollutants from Wastewaters*, CRC Press, Boca Raton, FL, 1996.
- [10] L. Jing-Fu, Z. Zong-Shan, J. Gui-Bin, Coating Fe₃O₄ magnetic nanoparticles with humic acid for high efficient removal of heavy metals in water, *Environ. Sci. Technol.* 42 (2008) 6949–6954.
- [11] H. Wang, Y. Jia, S. Wang, H. Zhu, X. Wu, Bioavailability of cadmium adsorbed on various oxides minerals to wetland plant species *Phragmites australis*, *J. Hazard. Mater.* 167 (2009) 641–646.
- [12] S. Yean, L. Cong, C.T. Yavuz, J.T. Mayo, W.W. Yu, A.T. Kan, V.L. Colvin, M.B. Tomson, Effect of magnetite particle size on adsorption and desorption of arsenite and arsenate, *J. Mater. Res.* 20 (2005) 3255–3264.
- [13] W. Tang, Q. Li, S. Gao, S.J. Ku, Arsenic (III, V) removal from aqueous solution by ultrafine α -Fe₂O₃ nanoparticles synthesized from solvent thermal method, *J. Hazard. Mater.* 192 (2011) 131–138.
- [14] G. Zelmanov, R. Semiat, Iron (Fe⁺³) oxide/hydroxide nanoparticles-based agglomerates suspension as adsorbent for chromium (Cr⁺⁶) removal from water and recovery, *Sep. Purif. Technol.* 80 (2011) 330–337.
- [15] R.M. Cornell, U. Schwertmann, *Iron Oxides in the Laboratory, Preparation and Characterization*, Wiley-VCH, Weinheim, 2000.
- [16] R.G. RuizMoreno, A.I. Martínez, R. Castro-Rodríguez, P. Bartolo, Synthesis and characterization of citrate coated magnetite nanoparticles, *J. Supercond. Novel Magn.* 26 (2013) 709–712.
- [17] R.G. RuizMoreno, A.I. Martínez, C. Falcony, R. Castro-Rodríguez, P. Bartolo-Pérez, M. Castro-Román, One pot synthesis of water compatible and monodisperse magnetite nanoparticles, *Mater. Lett.* 92 (2013) 181–183.
- [18] R. Massart, Preparation of aqueous magnetic liquids in alkaline and acidic media, *IEEE Trans. Magn.* 17 (1981) 1247–1248.
- [19] Environmental Protection Agency, *Determination of Metals and Trace Elements in Water and Wastes by Inductively Coupled Plasma-Atomic Emission Spectrometry*, EPA Method 200.7, Cincinnati, OH, 1994.
- [20] Y.S. Ho, Citation review of Lagergren kinetic rate equation on adsorption reactions, *Scientometrics* 59–1 (2004) 171–177.
- [21] Y.S. Ho, G. McKay, Application of kinetic models to the sorption of copper(II) on to peat, *Adsorpt. Sci. Technol.* 20 (2002) 797–815.
- [22] K.Y. Foo, B.H. Hameed, Insights into the modeling of adsorption isotherm systems, *Chem. Eng. J.* 156 (2010) 2–10.
- [23] J.A. López, F. González, F.A. Bonilla, G. Zambrano, M.E. Gómez, Synthesis and characterization of Fe₃O₄ magnetic nanofluid, *Rev. Latinoam. Metal. Mater.* 30–1 (2010) 60–66.
- [24] J. Hu, G. Chen, I.M.C. Lo, Removal and recovery of Cr(VI) from wastewater by maghemite nanoparticles, *Water Res.* 39 (2005) 4528–4536.
- [25] D.B. Singh, D.C. Rupainwar, G. Prasad, K.C. Jayaprakas, Studies on the Cd(II) removal from water by adsorption, *J. Hazard. Mater.* 60 (1998) 29–40.
- [26] S. Azizian, Kinetic models of sorption: A theoretical analysis, *J. Colloid Interface Sci.* 276 (2004) 47–52.

- [27] B. Benguella, H. Benaissa, Cadmium removal from aqueous solutions by chitin: Kinetic and equilibrium studies, *Water Res.* 36 (2002) 2463–2474.
- [28] A.B. Pérez-Marín, V.M. Zapata, J.F. Ortuño, M. Aguilar, J. Sáez, M. Lloréns, Removal of cadmium from aqueous solutions by adsorption onto orange waste, *J. Hazard Mater.* 139 (2007) 122–131.
- [29] R.D.C. Soltani, A.J. Jafari, Gh.S. Khorramabadi, Investigation of cadmium (II) ions biosorption onto pretreated dried activated sludge, *Am. J. Environ. Sci.* 5 (2009) 41–46.
- [30] S.R. Chowdhury, E.K. Yanful, Kinetics of cadmium(II) uptake by mixed maghemite–magnetite nanoparticles, *J. Environ. Manage.* 129 (2013) 642–651.
- [31] Y.S. Ho, G. McKay, Pseudo-second order model for sorption processes, *Process Biochem.* 34 (1999) 451–465.
- [32] N.K. Lazaridis, D.D. Asouhidou, Kinetics of sorptive removal of chromium(VI) from aqueous solutions by calcined Mg–Al–CO₃ hydrotalcite, *Water Res.* 37 (2003) 2875–2882.
- [33] Y.S. Ho, Review of second-order models for adsorption systems, *J. Hazard. Mater.* 136 (2006) 681–689.
- [34] H.K. An, B.Y. Park, D.S. Kim, Crab shell for the removal of heavy metals from aqueous solution, *Water Res.* 35 (2001) 3551–3556.
- [35] M. Namdeo, S.K. Bajpai, Investigation of hexavalent chromium uptake by synthetic magnetite nanoparticles, *Electron. J. Environ. Agric. Food. Chem.* 7–7 (2008) 3082–3094.
- [36] H. Karami, Heavy metal removal from water by magnetite nanorods, *Chem. Eng. J.* 219 (2013) 209–216.